Analysis Of DC-side Fault Response of MMCs with Controlled Fault Blocking Capability for Different Transmission Line Types

Willem Leterme*, Paul D. Judge† and Tim C. Green‡
*KU Leuven/EnergyVille, †The University of Edinburgh, ‡Imperial College London
*Kasteelpark Arenberg 10/Thor Park 8310, 3600 Genk
*3000 Leuven, 3600 Genk
Email: *willem.leterme@esat.kuleuven.be

Keywords

≪Converter Control≫, ≪Fault Handling Strategy≫, ≪HVDC≫, ≪Multilevel Converters≫.

Abstract

MMCs with controlled fault blocking capability retain control of their currents during a dc-side fault, thereby reducing the required interruption capabilities for switchgear. To design the dc-side control to achieve this capability, it is important to take into account the interaction between the converter control and the transmission line during a short-circuit on the transmission line. This paper uses a dc-side equivalent model to assess the interactions of the converter control for two types of converters, i.e., full-bridge and hybrid, with two main types of transmission lines during dc-side faults. In general, the dc-side voltages and currents for a full-bridge MMCs connected to an overhead line show more oscillatory behavior compared to an MMC connected to a cable. Furthermore, for some cases, a hybrid MMC connected to an overhead line may provide a more damped dc-side fault response due to its limited negative voltage capability.

Introduction

DC systems are increasingly used within the power system, with applications in High-, Medium- and Low Voltage dc (HVDC, MVDC and LVDC) [1]. In these systems, converters with fault blocking capability are considered attractive given that they can eliminate the need for dc-side switching equipment with fault interruption capability, as e.g., described in [2, 3] and used in a protection strategy as discussed in [4, 5]. In HVDC, modular multilevel converters (MMCs) with controlled fault blocking capability are planned for first installation in a German project connecting the north of the country to the south [6]. The increased use of these converters calls for a unified approach towards modeling the dc-side fault behavior, as detailed converter models are computationally inefficient and control details may not be available to the users of such converters or to suppliers of other equipments connected to these converters. In this paper, we analyze the influence of controller gains as well as transmission line type on the dc-side fault behavior of converters with controlled fault blocking capability using the modeling approach introduced in [7].

Modeling for DC-side Fault Analysis

In this paper, the dc EMT-type model as introduced and experimentally verified in [7] is used. This model only models the equivalent dc-side circuit of the converter (Fig. 1b). The model assumes variations in submodule voltages to be limited. As a consequence, energy balancing controls and submodule voltage balancing controls are not considered.

The dc EMT-type model uses the circuit as shown in Fig. 1b as the electrical model for the converter and only models the dc-side component of the current control. The converter is controlled using a discrete-time current control, which includes sensor and control delays, τ_m and τ_c. A limit is applied to the

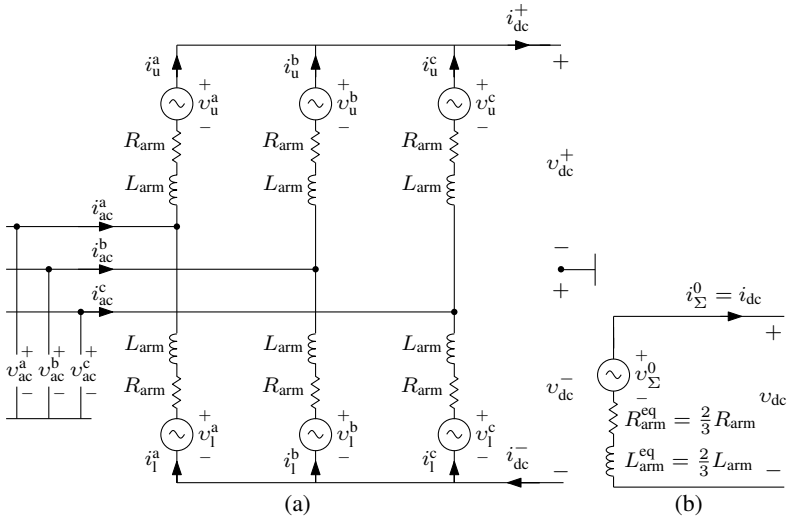

Fig. 1: MMC equivalent circuit diagram (a) and dc component (b) equivalent circuit diagrams.

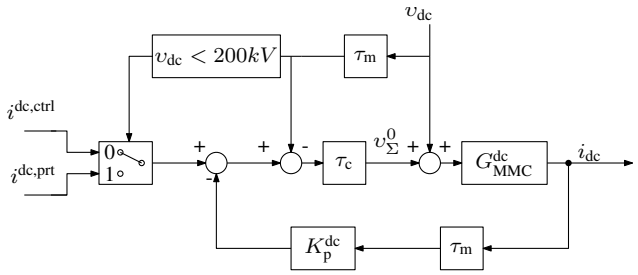

Fig. 2: Block diagram of converter dc-side current control and protection.

dc-side component of the voltage reference, to account for the limited voltage capability of the converter. A simplified version of the current control (without limit) is shown in Fig. 2. The equivalent RL-circuit shown in Fig. 1b is indicated by G_{MMC}^{dc}. The proportional constant of the feedback control is indicated by K_{p}^{dc}. The current reference is set from the control ($\tilde{i}^{\text{dc,ctr}}$) to the protection reference ($\tilde{i}^{\text{dc,prt}}$) based on an undervoltage criterion, but may also be based on an overcurrent criterion.

Although the dc EMT-type model only provides an approximation for the arm voltage limits, the model is used as it fits the purposes of the demonstration case studies. The purpose of the demonstration case studies are (i) to show the interactions between the converter control and transmission line type, and (ii) to demonstrate the differences between a hybrid and full-bridge MMC. The dc EMT-type model is able to demonstrate the differences qualitatively through the 'dc-side negative arm voltage limit', but more accurate models, such as the three-phase EMT-type model [7] or models such as the one introduced in [8] should be used to calculate these more accurately.

DC-side Fault Response Under Various Transmission Line Types

Case Study

To investigate the dc-side fault response, a case study is set up as shown in Fig. 3. The case study investigates three cases, namely, an MMC connected to a stiff dc voltage (i) directly, (ii) through a cable and (iii) through an overhead line. The MMC parameters are based on the ones given in Table I and the overhead line and cable parameters are given in Table II. The cables are buried 1 m below ground and the ground resistivity is 0.5 Ω·m. To investigate the effect of close-up and remote faults, the transmission line length is varied between 25 km and 300 km. The considered sensor and actuator delays are 100 μs each, taking a value close to the ones found in [3]. The converter negative voltage capability is assumed to be -650 kV in case of the full-bridge MMC and -325 kV in case of the hybrid MMC. The proportional

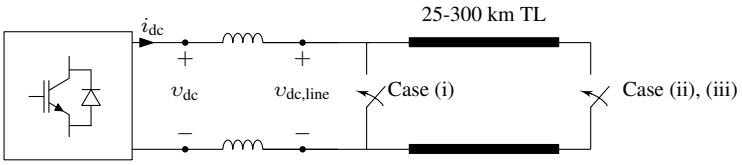

Fig. 3: Case Study Setup

Table I: Converter Parameters

Parameter	Value
Rated dc power	960 MW
dc nominal pole-to-pole voltage	640 kV
dc negative voltage capability (full-bridge)	-650 kV
dc negative voltage capability (hybrid)	-325 kV
Arm inductance L_{arm}	0.05 H
Arm resistance R_{arm}	1.6 Ω

Table II: Overhead line and cable parameters.

Parameter	Value
No. of conductors	2
Configuration	Horizontal
Conductor spacing	13.4 m
Conductor height	25 m
Conductor sag	13.9 m
Conductor outer radius	1.62 cm
Conductor DC resistance	51.9 mΩ/km
Ground resistivity	50 Ω·m

Conductor	Outer Radius [mm]	ρ [$\Omega \cdot m$]	μ_r	ε_r
Core	25.13	1.72e-8	1	-
Insulation	48.38	-	-	2.3
Screen	54.13	21.4e-8	1	-
Insulation	54.13	-	-	2.3
Armor	59.73	1.38e-7	-	10
Insulation	64.73	-	-	2.3

feedback of the dc-side current control is varied between 10 and 150, with intermediate steps taken as multiples of 50. The study case is modeled in PSCAD, where a timestep of 10 μs is chosen for the simulation.

The transmission lines are modeled using a frequency-dependent phase model. To obtain a stable simulation, in the case of an overhead line, capacitors were put at the dc terminal, with a capacitance-to-ground of 1 μF.

Results

Effect of dc-side proportional control on Full-Bridge Response

The dc-side fault response for each of the three cases differs according to the influence of the converter current control on the dc-side voltage. For a stiff voltage source (case (i), no transmission line), the converter current control has no influence on the dc-side voltage. The dc-side fault current shows a uniformly decaying behavior for all K_{p}^{dc}, except for $K_p = 150$, where the dc-side fault current undershoots before reaching zero (see Fig. 4). For the cable (case (ii)), the dc-side voltage decays more slowly due to the capacitance of the cable, and oscillates around zero before reaching steady state. The dc-side fault current increases to a lower value compared with the stiff voltage source, and also shows oscillatory behavior before reaching zero. In the overhead line case, the converter current control has the largest impact on the dc-side voltage. The dc-side voltage shows the most oscillatory behavior of the three cases. The peak current is the lowest of all cases, as it is limited by the line inductance, but like the dc-side voltage, it shows the most oscillatory behavior of the three cases.

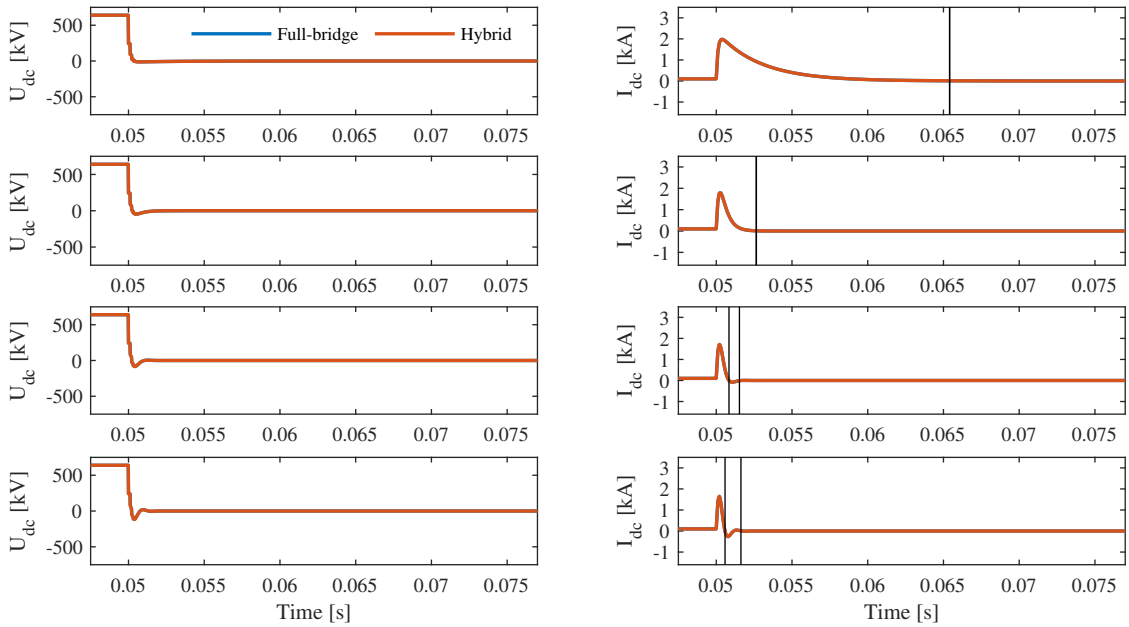

Fig. 4: Dc-side fault response for stiff dc voltage case (upper to lower plot: $K_p = 10, 50, 100, 150$). The solid black lines represent the "rise" and "settling" times, respectively.

In the following paragraphs, the influence of the dc-side proportional constant, $K_{\mathrm{p}}^{\mathrm{dc}}$, on three parameters is analyzed. A first parameter of interest is the time until the fault has reached a value at which it can be interrupted by switchgear without fault current interruption capability. To characterize this, a "rise time" and "settling time" are defined as the first instant at which the current falls below 0.01 kA and the instant at which the current permanently remains below 0.01 kA, respectively. The second parameter of interest is the peak dc-side fault current, and the third parameter of interest is the peak value of the dc-side voltage.

For cases (i) and (ii), in general, the settling time of the current decreases as $K_{\mathrm{p}}^{\mathrm{dc}}$ increases, although this trend is only valid for $K_{\mathrm{p}}^{\mathrm{dc}} < 150$ (see Fig. 4, Fig. 5 and Fig. 6). For case (iii), the value of $K_{\mathrm{p}}^{\mathrm{dc}}$ leading to the minimum settling time of the current depends on the length of the transmission line. For the cases of 25 km and 300 km, the settling time is the lowest for $K_{\mathrm{p}}^{\mathrm{dc}} = 50$ and 10, respectively. In general, increasing $K_{\mathrm{p}}^{\mathrm{dc}}$ leads to an increased number of oscillations in the cases with $K_{\mathrm{p}}^{\mathrm{dc}}$ above 50. In conclusion, for a stiff voltage source and a cable, increasing $K_{\mathrm{p}}^{\mathrm{dc}}$ has in general a positive effect on the rise and settling times. For overhead line case, increasing $K_{\mathrm{p}}^{\mathrm{dc}}$ leads to a lower rise time, whereas the settling time in general increases.

The peak dc-side fault current, a second parameter of interest, shows different behavior for each of the cases. Using this model setup, for all cases, the peak fault current decreases with an increase in $K_{\mathrm{p}}^{\mathrm{dc}}$. Using the equivalent diagram of Fig. 1b, it can be seen that the dc-side current increases whenever $\upsilon_{\Sigma}^{0} > \upsilon_{\mathrm{dc}}$ and vice versa. The dc-side current controller may set υ_{Σ}^{0} below υ_{dc} even during the increase of the dc-side fault current. This is more effective for remote faults in the cable case compared with the overhead line case, as can be seen when comparing Fig. 6 and 8.

The third parameter to take into account is the dc-side voltage. In the second and third case, the current controllers may influence the dc-side voltage, as can be seen in Fig. 5 and Fig. 7. For the cable case, the value of $K_{\mathrm{p}}^{\mathrm{dc}}$ has only a minor effect on the dc-side voltage. In the overhead line case, the current controller has a significant impact on the dc-side voltage in terms of absolute peak voltage and oscillatory behavior. For the lowest $K_{\mathrm{p}}^{\mathrm{dc}}$, the peak voltage and number of oscillations remain limited. For the highest $K_{\mathrm{p}}^{\mathrm{dc}}$, the peak voltage may increase slightly beyond the maximum voltage and oscillatory behavior is at its worst. In conclusion, for the overhead line case, increasing $K_{\mathrm{p}}^{\mathrm{dc}}$ may not have the overall beneficial effect as seen in the case with the stiff dc-side voltage.

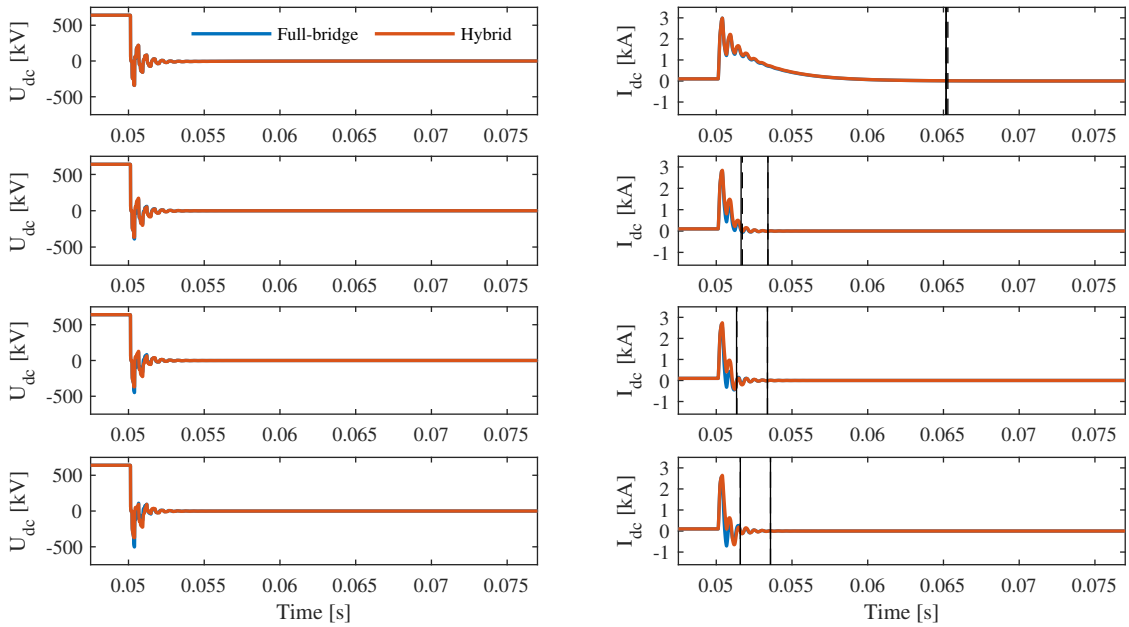

Fig. 5: Dc-side fault response for 25 km cable case (upper to lower plot: $K_p = 10, 50, 100, 150$). The solid and dashed black lines represent the "rise" and "settling" times for the full-bridge and hybrid case, respectively.

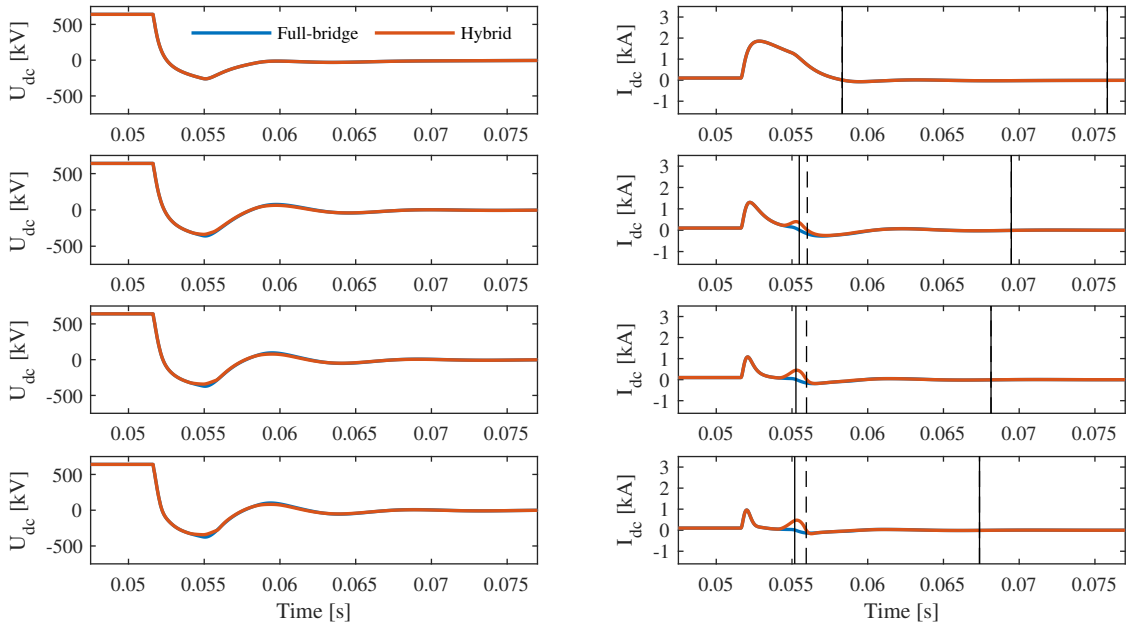

Fig. 6: Dc-side fault response for 300 km cable case (upper to lower plot: $K_p = 10, 50, 100, 150$). The solid and dashed black lines represent the "rise" and "settling" times for the full-bridge and hybrid case, respectively.

Difference between full-bridge and hybrid MMC

For case (i), i.e., the converter connected to a stiff dc-side voltage source, there is no difference between the responses of the full-bridge and the hybrid MMC (see Fig. 4). In this case, the negative voltage capability limit is not reached for any of the proportional control constants. As such, there is no difference in the current control response between the two cases.

In case the converter is connected to a cable, the full-bridge converter outperforms the hybrid converter in controlling the dc-side current, but there is very little difference between the rise and settling times.

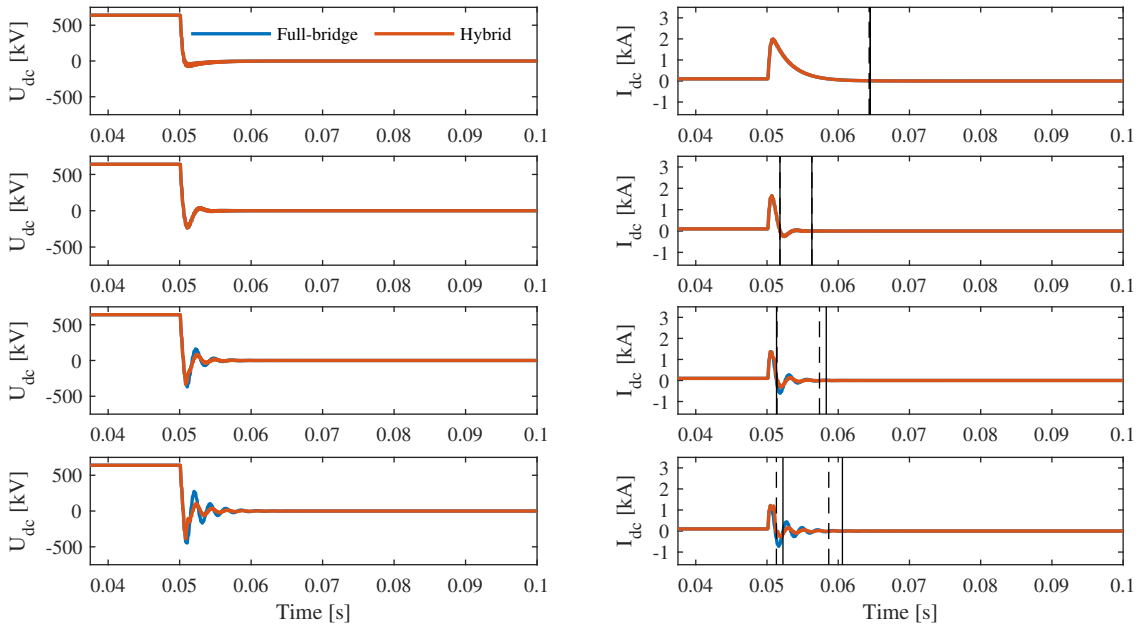

Fig. 7: Dc-side fault response for 25 km overhead line case (upper to lower plot: $K_p = 10, 50, 100, 150$). The solid and dashed black lines represent the "rise" and "settling" times for the full-bridge and hybrid case, respectively.

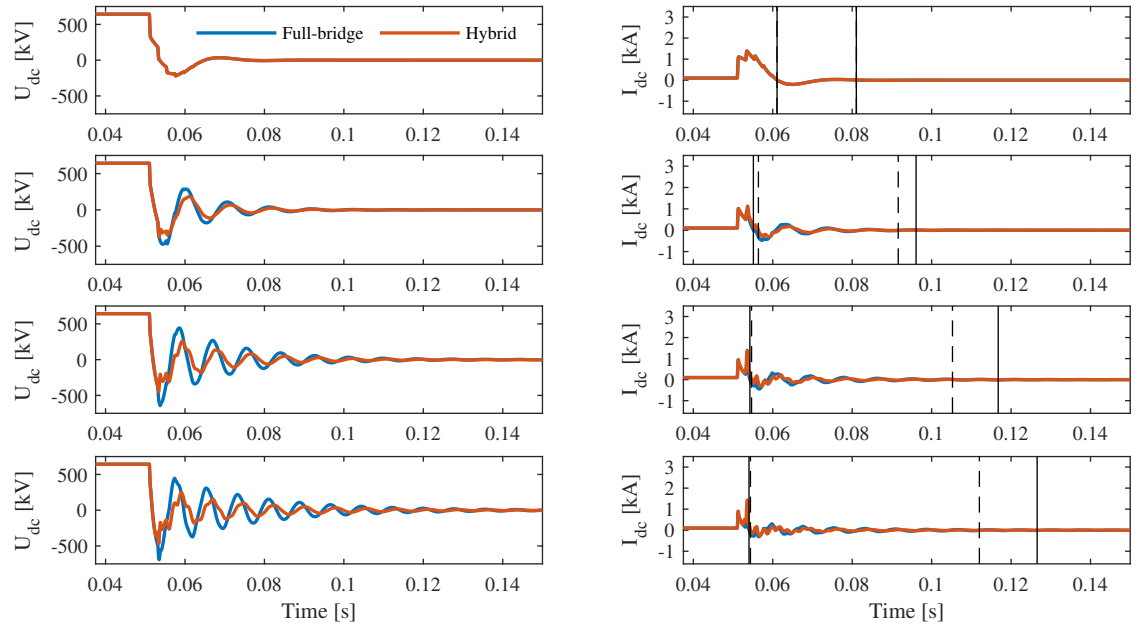

Fig. 8: Dc-side fault response for 300 km overhead line case (upper to lower plot: $K_p = 10, 50, 100, 150$). The solid and dashed black lines represent the "rise" and "settling" times for the full-bridge and hybrid case, respectively.

The dc-side current of the full-bridge MMC always lies below the one of the hybrid MMC (Fig. 5 and 6). This is due to the fact that the full-bridge retains full control of its dc-side current given that the dc-side voltage never falls below its negative voltage capability. By contrast, the hybrid MMC loses control of its dc-side current whenever it cannot generate a dc-side voltage lower than the one resulting from the fault. At those instants, the dc-side current shows a temporary uncontrolled increase (e.g., see Fig. 6 for $K_{\mathrm{p}}^{\mathrm{dc}} > 50$). The difference in rise times is in the order of one millisecond and in most cases, there is no difference in settling times.

For the case where the converter is connected to an overhead line (case (iii)), the converter response

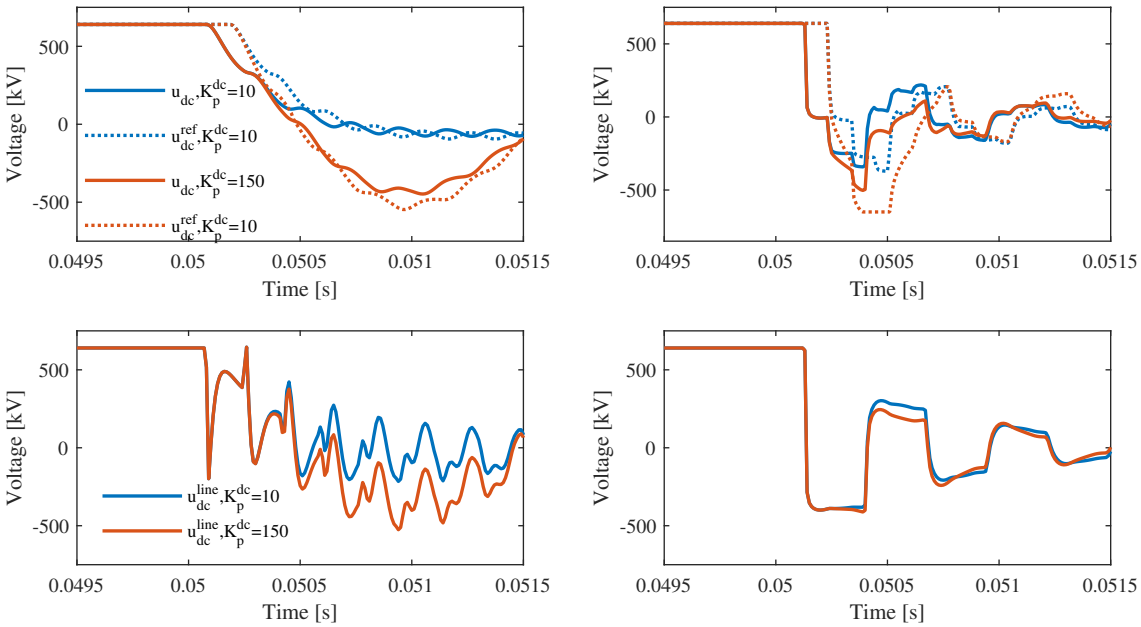

Fig. 9: DC-side fault response of full-bridge for 25 km overhead line case (left) and 25 km cable case (right).

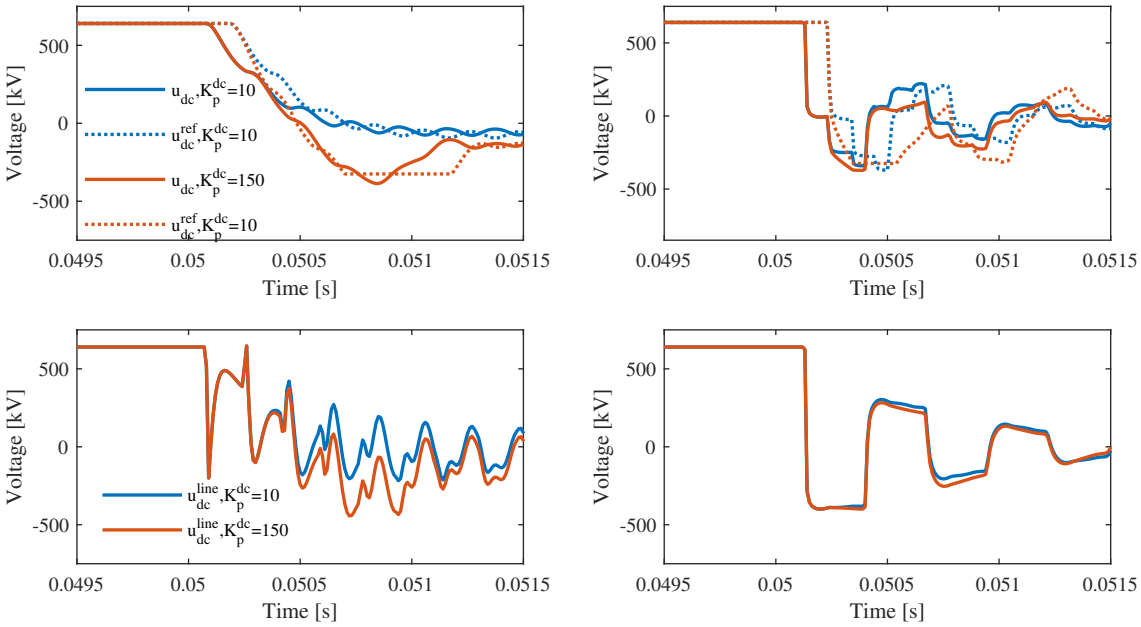

Fig. 10: DC-side fault response of hybrid MMC for 25 km overhead line case (left) and 25 km cable case (right). Voltage reference input shown in dashed lines.

should be considered distinctly for the cases in which the line length is 25 km and 300 km. In case the line length is 25 km (Fig. 7), the voltages and currents as generated by the hybrid MMC are considerably less oscillatory compared with those generated by the full-bridge MMC. This reduction in oscillatory behavior, especially at high K_p^{dc}, may be attributed to the fact that the hybrid MMC is forced to retain the voltage at its negative arm voltage limit for a certain amount of time. This seems to have a damping effect on dc-side voltages and currents, causing the fault current to decay more quickly. In case the line length is 300 km, the above described effect plays a lower role and both responses show oscillatory behavior. In all cases with K_p^{dc} >50, the amplitude of the voltage oscillations is higher for the full-bridge MMC in comparison with the hybrid MMC (Fig. 8).

Control response during DC-side faults

The origin of the oscillations in the DC-side fault response is different for the overhead line-case and the cable case.

For the overhead line case, the (zero-crossing) oscillations visible in Fig. 7 and Fig 8 for $K_{\mathrm{p}}^{\mathrm{dc}}$ beyond 100 and 50, respectively, are linked to interactions between the converter control and the overhead line, but are not directly linked to reflections of traveling waves originating from the fault. In this case, the traveling wave reflections appear as small ripples superimposed to the lower frequency oscillation (Fig. 9, left plots). For the case of $K_{\mathrm{p}}^{\mathrm{dc}} = 150$, the succession of incoming waves and the delayed control response cause a cascading effect which initially pushes the dc-side voltage downwards and triggers the large oscillation. In case of a low proportional constant, and hence a less agressive response of the controller, these oscillations do not occur. In case of a hybrid MMC, the oscillations are damped even for high proportional constants, given that the negative voltage limit is hit in an earlier stage, resulting in a reduced magnitude of oscillations compared to the full-bridge case (see Fig. 10 and 8).

For the cable-case, the zero-crossing oscillations more closely follow the reflection pattern of the traveling waves generated by the fault (Fig. 9, right plots). The voltage reference takes a similar shape as the dc-side voltage, with a delay of 200 μs due to control and sensor delays. Given that the cable represents a more stiff voltage in comparison to the overhead line, the converter control has a relatively low influence on the shape of the DC-side voltage. In contrast with the overhead line case, the lower negative arm voltage limit of the hybrid MMC does not seem to have a beneficial effect in damping the oscillations.

Conclusion

The response of an MMC with controlled fault blocking capability depends on the transmission line type it is connected to and its negative voltage capability. This paper has used a relatively simple, but experimentally verified, dc-side equivalent with proportional feedback control in a preliminary analysis of the dc-side fault response of an MMC with controlled fault blocking capability connected to an overhead line or cable. For a full-bridge MMC connected to a cable, an increase in the proportional feedback gain leads to a lower settling time and a lower peak fault current. For a full-bridge MMC connected to an overhead line, an increase in the proportional feedback gain leads to a lower peak fault current, but may lead to oscillatory behavior which results in a longer settling time. Furthermore, in the latter case, the dc-side voltage may reach unwanted high values due to the influence of the dc-side current controller on its relatively weak dc-side terminal voltage. The analysis showed that the oscillations observed in the overhead line may be attributed to interactions of the converter control with the transmission line. By contrast, the oscillations observed in the cable case may be attributed to reflections of traveling waves initiated by the fault. As a final note, a hybrid MMC connected may provide a more damped response compared to a full-bridge MMC when it is connected to an overhead line.

References

[1] M. Barnes, D. Van Hertem, S. P. Teeuwsen, and M. Callavik, "HVDC Systems in Smart Grids," *Proceedings of the IEEE*, vol. 105, no. 11, pp. 2082–2098, Nov. 2017.

[2] R. Marquardt, "Modular Multilevel Converter topologies with DC-Short circuit current limitation," in *Proc. IPEC 2011 - ECCE Asia*, Jeju, South Korea, Jun. 2011, pp. 1425–1431.

[3] M. Winkelnkemper, L. Schwager, P. Blaszczyk, M. Steurer, and D. Soto, "Short circuit output protection of MMC in voltage source control mode," in *Proc. 2016 IEEE-ECCE*, Milwaukee, WI, USA, Sep. 2016, 6 pages.

[4] P. Cairoli, R. A. Dougal, U. Ghisla, and I. Kondratiev, "Power sequencing approach to fault isolation in dc systems: Influence of system parameters," in *Proc. 2010 ECCE*, Atlanta, GA, Sep. 2010, pp. 72–78, 7 pages.

[5] P. Ruffing, C. Brantl, C. Petino, and A. Schnettler, "Fault current control methods for multi-terminal DC systems based on fault blocking converters," *The Journal of Engineering*, vol. 2018, no. 15, pp. 871–875, 2018.

[6] J. Dorn, P. La Seta, F. Schettler, J. Stankewitz, M. vor dem Berge, R. Teixeira Pinto, K. Uecker, M. Walz, K. Vennemann, B. Rusek, J. Reisbeck, and C. Butterer, "Full-bridge VSC: An essential enabler of the transition to an energy system dominated by renewable sources," in *Proc. IEEE PES GM*, Boston, MA, Jul. 2016, 5 pages.

[7] W. Leterme, P. D. Judge, J. Wylie, and T. C. Green, "Modeling of MMCs With Controlled DC-Side Fault-Blocking Capability for DC Protection Studies," *IEEE Transactions on Power Electronics*, vol. 35, no. 6, pp. 5753–5769, Jun. 2020.

[8] H. Saad, K. Jacobs, W. Lin, and D. Jovcic, "Modelling of MMC including half-bridge and Full-bridge submodules for EMT study," in *2016 Power Systems Computation Conference (PSCC)*, Jun. 2016, pp. 1–7.